Journal of Energy Storage 44 (2021) 103292

Contents lists available at ScienceDirect

Journal of Energy Storage

journal homepage: www.elsevier.com/locate/est

A data-driven accurate battery model to use in probabilistic analyses of power systems

Md. Kamruzzaman [a,b], Xiaohu Zhang [b,*], Michael Abdelmalak [a], Di Shi [b], Mohammed Benidris [a]

[a] Department of Electrical and Biomedical Engineering, University of Nevada, Reno, NV 89557–0260, USA
[b] GEIRI North America, San Jose, CA, USA

ARTICLE INFO

Keywords:
Battery model
Genetic algorithm
Neural network
Optimal locations
Power system reliability

ABSTRACT

Analytical battery models depend on a set of complex nonlinear equations that make them impractical to use in probabilistic analyses (e.g., reliability evaluation) of power systems. Machine-learning algorithms have the potential to reduce or even avoid the computational complexities of incorporating actual battery characteristics in probabilistic analyses. In this paper, a neural network (NN)-based approach is proposed to develop a battery model that captures the non-linear interactions between charging/discharging power and battery state of charge (SoC). In the proposed approach, an NN with a rectified linear unit activation function is trained using historical data generated from an experimentally validated battery model. Another NN with linear activation function is trained to capture the relationship between charging/discharging power limits and SoC. Weights and biases of the trained networks in conjunction with mixed integer linear programming are used to develop an accurate and computationally attractive battery model. Also, a mathematical model is formulated to accommodate the proposed battery model in power system reliability evaluation. Moreover, a genetic algorithm-based approach is used to determine optimal locations for batteries considering the developed model to enhance reliability of power systems. The proposed approach is demonstrated on a modified version of the IEEE 33-bus distribution system. Monte Carlo simulation is performed to calculate reliability indices. The results show that the proposed battery model is effective to incorporate actual battery characteristics in probabilistic analyses (evaluating reliability and finding optimal battery locations) of power systems.

1. Introduction

The deployment of energy storage devices (ESDs) in power systems has increased significantly to provide both operational (e.g., to maintain or increase stability or reliability of power systems) and ancillary services (e.g., frequency regulation or operating reserve in electricity market) of power grids. With the increasing deployment of ESDs, incorporating accurate battery models in probabilistic analyses of power systems has gained significant importance to allocate them properly for enhancing their efficiency in providing grid support. However, the use of analytical/experimental battery models in probabilistic analysis of power systems has become a bottleneck due to the heavy computational burden associated with the requirement of solving a set of nonlinear equations for a large number of iterations. Ideal battery models have been commonly used in probabilistic analysis of power systems. Although the use of ideal battery models in power system problems reduces the computational burden, inaccuracies remains in the obtained results due to the consideration of constant charging/discharging efficiency, which may increase the investment or decrease the battery performance significantly.

Machine learning (ML) algorithms can be a promising solution to reduce computational burden of capturing non-linear battery characteristics in probabilistic analyses. For instance, neural networks (NNs) can be trained to capture the relationships between charging/discharging power and battery state of charge (SoC) without solving non-linear equations. Therefore, developing ML-based accurate battery models is indispensable to overcome the computational barrier of using accurate battery models in power system planning studies.

Several studies have focused on providing a proper battery model under a wide range of considerations. Review of the state-of-the-art in the field of battery modeling has been provided in [1]. Authors of [2–5] have proposed several analytical methods to calculate battery circuit parameters (i.e., resistance, capacitance, and open circuit voltage). Also, a comprehensive battery model considering electrochemical properties has been developed and experimentally validated in [6]. Focusing

* Corresponding author.
E-mail addresses: mkamruzzaman@nevada.unr.edu (M. Kamruzzaman), youwen9h@gmail.com (X. Zhang), mabdelmalak@nevada.unr.edu (M. Abdelmalak), sdxjtu@gmail.com (D. Shi), mbenidris@unr.edu (M. Benidris).

https://doi.org/10.1016/j.est.2021.103292
Received 23 May 2021; Received in revised form 3 September 2021; Accepted 20 September 2021
Available online 13 October 2021

on the trade-off between speed and accuracy, several types of battery circuit models have been studied, which facilitate the selection process of a certain model for a specific task [7]. A procedure to experimentally validate the relationship between charge/discharge capabilities and SoC of different types of batteries has been proposed in [8]. In [9], an improved deep learning-based method has been proposed to determine battery SoC that is applicable in electric vehicles. A convolutional NN and a long short-term memory method have been used to predict the remaining battery lifetime in [10]. A coupled cation–vacancy pair in Ni-doped CoSe has been introduced in [11] to boost hydrogen evolution reaction activity, which provides guidance to design new electrocatalysts. In [12], a Fe-incorporated topochemical deintercalation-based redesign method has been used to improve intrinsic activity of six-coordinated octahedrons in Co_9S_8. $RhSe_2$ has been reported as a "3D" electrocatalyst for hydrogen evolution reaction with top-class activity in [13], which is synthesized using a facile solid-state method. In [14], graphene-like $Co_{0.85}Se$ has been doped with sulfur to enhance hydrogen evolution reaction (HER) in electrocatalytic, which inspires for intrinsic HER activity optimization of other similar transition metal chalcogenides. The pulse laser ablation in air (LAA) has been employed in [15] to modify several features of energy-related catalytic reactions such as morphology modulation, defects engineering, or heterojunction fabrication. Although each proposed model has its own advantages and disadvantages, reducing the complexity of using battery model in probabilistic analyses of power systems is still under investigation. Therefore, it is imperative to develop an accurate battery model that can be used to incorporate the non-linear relationship between charging/discharging power and energy level of batteries in probabilistic analyses of power systems.

Several battery models have been proposed [2–10] to capture the physical interactions within a battery unit; however, each model is built based on various assumptions to reduce the complexity of nonlinear phenomena. Selecting a proper model for a specific power system study always exhibits a trade-off between efficiency, accuracy, and complexity [16]. Analytical battery models are highly complex yielding increased computational burden [17] especially for time involved problems such as reliability evaluation of electric power systems. In [18], an ideal battery model with constant charging/discharging rates has been used to analyze the impacts of dynamic thermal rating and battery energy storage systems on reliability of wind-integrated power systems. A multiobjective framework considering an ideal battery model has been proposed in [19] to optimize uprating of real-time thermal rating of lines and capacity of battery energy storage systems against wind curtailment, network aging and reliability. In [20], a method considering ideal batter models has been proposed to analyze the combined effects of battery energy storage systems, demand response, and dynamic thermal rating on reliability of power systems. Although the proposed approaches in [18–20] have provided insights into improving power system reliability using battery storage systems, these approaches considered ideal battery models where charging/discharging rates are constant. However, in the practical scenario, discharging efficiency is low for high current value and low SOC (can be dropped up to 33% from the maximum value) [6,17]. Also, the charging efficiency follows a nonlinear behavior with a smaller efficiency dropping in the smaller operating region [6,17]. Therefore, use of actual charging/discharging efficiencies of batteries is necessary to improve accuracy of evaluating and enhancing power system reliability with battery energy storage systems. Thus, it has become important to have an accurate battery model that captures non-linear interactions between charging/discharging power and SoC of batteries in power system reliability enhancement studies.

Optimal deployment of battery energy storage systems (BESSs) in power systems has gained significant momentum to improve the overall performance of power systems. An ideal battery model under constant charging/discharging rates has been used in [21] to determine optimal locations and sizes for batteries to improve load factor of power systems. Impacts of different constant charging/discharging rates on supply, bidding, optimal scheduling, and optimal siting of batteries have been analyzed in [22]. An strategy to determine optimal battery locations has been proposed in [23] to maintain voltage limits of distribution systems integrated with photovoltaic generators. Several ideal battery model-based optimal battery siting strategies have been proposed to improve voltage profile of power systems considering battery lifespan [24], load-sensitivity [25], and cost reduction [26]. In [27], a method to determine optimal battery locations considering ideal battery models has been proposed to enhance reliability of solar-integrated power systems. A method to quantify the sizes of battery energy storage devices using ideal battery model has been proposed in [28] to reduce the negative impacts of wind energy on power systems. Although BESSs have been used in a wide range of applications, their potential use to increase the reliability of power systems has not been explored comprehensively. In addition, most of the studies have relied on ideal battery models to reduce the computational burdens ignoring the impacts on accuracy of obtained results. Thus, a method to determine optimal battery locations based on an accurate battery model to maximize power system reliability with high accuracy needs to be developed.

In this paper, a data-driven accurate battery model is developed to capture non-linear characteristics of batteries without solving non-linear equations. In the proposed approach, an NN with a rectified linear unit activation function (ReLU) is trained to capture the non-linear relationship between charging/discharging power and energy level of batteries. Another NN with linear activation function is trained to establish the relationship between charging/discharging power limits and SoC. A historical data set to train both NNs is generated using an experimentally validated battery model in [6]. The weights and biases of the trained networks in conjunction with mixed integer linear programming (MILP) are used to develop the proposed accurate battery model. A linearized AC power flow model is leveraged to integrate the proposed battery model in power system reliability evaluation. Optimal locations for batteries considering the developed model is determined using a genetic algorithm (GA) to enhance reliability of power systems. Main contributions of the proposed work in comparison with existing methods are summarized as follows.

- The proposed data-driven battery model is effective in removing the computational issues of incorporating the actual/experimental relationship between charging/discharging power and SoC levels of batteries in probabilistic analysis of power systems, which is beneficial to enhance the accuracy of power system planning studies for battery energy storage systems.
- NNs are trained to capture the relationship between charging/discharging power and energy and charging/discharging power limits and SoC of batteries. Weights and biases of the trained networks and MILP are used to formulate a mathematical model for the proposed battery model, which is used to develop a framework for integrating actual battery characteristics in power system reliability evaluation using a linearized AC power flow. The developed framework eliminates the scalability issues of incorporating actual battery characteristics in reliability studies of large integrated power grids by removing the requirement of solving computationally expensive AC optimal power flow for a large number of iterations.
- A GA-based algorithm is proposed to provide a guideline for incorporating the proposed accurate battery model in determining optimal battery locations to enhance power system reliability.

The effectiveness of the proposed approach is demonstrated on a modified version of the IEEE 33-bus distribution system. Monte Carlo simulation is performed to calculate reliability indices.

The rest of the paper is arranged as follows. Section 2 describes the proposed battery modeling approach. Section 3 illustrates the integration strategy of battery model into reliability evaluation problem. Section 4 provides a description of the optimal siting strategy for reliability enhancement. Section 5 demonstrates the proposed method using numerical examples. Section 6 provides several concluding remarks.

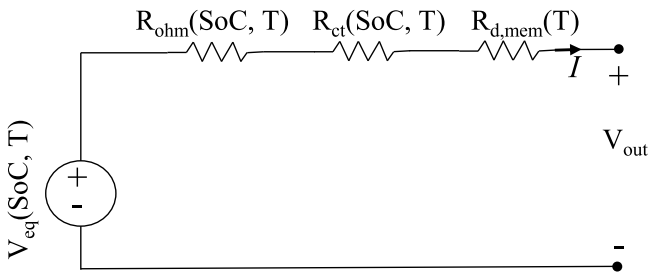

Fig. 1. Battery Equivalent Circuit Model.

2. The proposed data-driven accurate battery model

The proposed approach to develop data-driven battery model has three main steps, which are as follows: collect historical data to train the NNs, perform training of the NNs using historical data, and extract the weights and biases of the trained networks in conjunction with mixed integer linear programming to develop the accurate battery model. These steps are described in the following subsections.

2.1. Data generation scheme

In this paper, an experimentally validated battery model provided in [6] is used to generate training data for the proposed battery model. Fig. 1 shows the equivalent circuit of this battery model.

The equivalent circuit model contains a voltage source and three resistors that represent three electrochemical processes, which are ohmic losses, charge transfer, and membrane diffusion. In [6], a mathematical model based on the equivalent circuit model of Fig. 1 has been developed to express the non-linear relationships between charging/discharging power and SoC. Instead of reproducing the complex mathematical representation, only the required expressions for this work are provided next.

2.1.1. The voltage source

The expression for the equivalent voltage is as follows.

$$V_{eq} = U^{o}_{bat} + \frac{R_g \cdot T}{F} \cdot \ln\left(\frac{(1-\mathcal{X}_{cd})\cdot \mathcal{X}_{ad}}{\mathcal{X}_{cd}\cdot(1-\mathcal{X}_{ad})}\right) + v_{int} \tag{1}$$

where U^{o}_{bat} is the reference potential at equilibrium; R_g is the gas constant; F is the Faraday constant; T is the temperature; $\mathcal{X}_{cd}$ and $\mathcal{X}_{ad}$ are the molar fractions of cathode and anode, respectively; v_{int} is the non-ideal interaction voltage; and V_{eq} is the equilibrium voltage of the battery. The expressions for the $\mathcal{X}_{cd}$, $\mathcal{X}_{ad}$, and v_{int}, in terms of SoC, are as follows,

$$\mathcal{X}_{ad} = 0.083 + 0.917 \cdot SoC, \tag{2}$$

$$\mathcal{X}_{cd} = 1 - 0.7 \cdot SoC, \tag{3}$$

$$v_{int} = v_{int,cd} - v_{int,ad}, \tag{4}$$

$$v_{int,i} = \sum_{j=o}^{7} A_j \left[(2\mathcal{X}_i - 1)^{j+1} - \frac{2\mathcal{X}_i \cdot j \cdot (1-\mathcal{X}_i)}{(2\mathcal{X}_i - 1)^{1-j}}\right], \tag{5}$$

where A_j is the interaction parameters for seventh order Redlich–Kister equation and $i = cd, ad$, where cd denotes cathode and ad denotes anode.

2.1.2. The equivalent resistances

The expressions for ohmic losses, charge transfer, and membrane diffusion are as follows.

- Ohmic losses

$$R_{ohm} = R_{ohm,0} + R_{ohm,T} \cdot T + R_{ohm,SoC} \cdot SoC \tag{6}$$

where $R_{ohm,0}$, $R_{ohm,T}$, and $R_{ohm,SoC}$ are the parameters to obtain resistance using ohmic phenomena.

- Charge transfer

$$R_{ct} = \frac{1}{(\mathcal{X}_{cd}\cdot\mathcal{X}_{ad})^{0.5}} \cdot \left[\frac{R_g \cdot T \cdot e^{(E_A/R_g\cdot T)}}{F^2 \cdot A_{SEI} \cdot k_0}\right] \tag{7}$$

where A_{SEI} is the solid electrolyte interface area; E_A is the activation energy; and k_0 is the reaction rate constant.

- The membrane diffusion

$$R_{d,mem} = K_{d,mem} \cdot \exp\left(\frac{b_{d,mem}}{T - T_{0,d,mem}}\right) \tag{8}$$

where $K_{d,mem}$, $b_{d,mem}$, and $T_{0,d,mem}$ are the membrane diffusion constants.

The resultant equivalent resistance for all the losses of the battery circuit model, R_{tot}, is as follows.

$$R_{tot} = R_{ohm} + R_{ct} + R_{d,mem}, \tag{9}$$

From the equivalent circuit model, the discharging efficiency is calculated as follows.

$$\eta^{dis} = \frac{P^{dis}}{P^{out}} = 1 - \frac{I \cdot R_{tot}}{V_{eq}}, \tag{10}$$

where P^{out} is the outgoing power from battery; P^{dis} is the discharged power to the grid; I is the discharging/charging current of the battery equivalent circuit model; and η^{dis} is the discharging efficiency.

Similarly, the expression for the charging efficiency is represented as follows.

$$\eta^{ch} = \frac{P^{in}}{P^{ch}} = 1 - \frac{V_{eq}}{V_{eq} + I \cdot R_{tot}}, \tag{11}$$

where P^{ch} is the outgoing charging power from grid; P^{in} is the incoming power to the battery; and η^{ch} is the charging efficiency.

Finally, the relationship between battery energy level and charging/discharging power is expressed as follows.

$$E_t = E_{t-1} + \eta^{ch}_{t-1} P^{ch}_{t-1} - \frac{1}{\eta^{dis}_{t-1}} P^{dis}_{t-1}, \tag{12}$$

Subject to,

$$E^{\min}_t \le E_t \le E^{\max}_t, \tag{13}$$

$$0 \le P^{ch}_t \le P^{ch,\max}_t, \tag{14}$$

$$0 \le P^{dis}_t \le P^{dis,\max}_t, \tag{15}$$

$$SoC_t = \frac{E_t}{E^c_t}, \tag{16}$$

where t represents the time step; E_{t-1} is the energy level at previous time step; E_t is the energy level at current time step; $E^{\min}_t$ and $E^{\max}_t$ are the minimum and maximum allowable energy level of the battery; E^c_t is the battery capacity; $P^{ch,\max}_t$ and $P^{dis,\max}_t$ are the maximum charging and discharging power limits at current time step, respectively; and SoC_t is the state of charge at current time step.

The mathematical expressions to determine the charging/discharging power limits are taken from [17] and expressed as follows.

$$P^{ch,\max}_t = V_{eq,t} \cdot I^{ch,\max}_t + (I^{ch,\max}_t)^2 \cdot R_{tot} \tag{17}$$

$$P^{dis,\max}_t = V_{eq,t} \cdot I^{dis,\max}_t - (I^{dis,\max}_t)^2 \cdot R_{tot} \tag{18}$$

where $I_t^{ch,\max}$ and $I_t^{dis,\max}$ are the maximum charging and discharging current. Further illustration to calculate $I_t^{ch,\max}$ and $I_t^{dis,\max}$ in terms of SoC has been provided in [17].

The expressions provided in (1)–(18) are used to generate training data for the proposed battery model. The procedure to select input and output (target) parameters as well as NNs training are described in the following subsection.

2.2. Training neural networks to capture actual battery characteristics

The relationship between charging/discharging power and battery energy level follows a non-linear behavior, whereas the relationship between charging/discharging power limits and SoC exhibits a linear behavior for a wide range of SoC levels (25%–95%). Therefore, an NN with ReLU activation function is used to capture the non-linear behavior whereas another NN with linear activation function is used to capture the linear behavior.

2.2.1. Training algorithm for the NN with ReLU activation function to capture relationship between energy level and charging/discharging power

The input training matrix, X, to capture the relationship between charging/discharging power and energy level is provided as follows.

$$X = \begin{bmatrix} x^1 & x^2 & \cdots & x^n \end{bmatrix}^{T_r} = \begin{bmatrix} E_{t-1}^1 & P_{t-1}^{ch,1} & P_{t-1}^{dis,1} \\ E_{t-1}^2 & P_{t-1}^{ch,2} & P_{dis,2}^{t-1} \\ \vdots & \vdots & \vdots \\ E_{t-1}^n & P_{t-1}^{ch,n} & P_{t-1}^{dis,n} \end{bmatrix}, \tag{19}$$

where x^n represents the nth training sample; E_{t-1}^n, $P_{t-1}^{ch,n}$, and $P_{t-1}^{dis,n}$ are the energy level, charging power, and discharging power, respectively, at previous time step for the nth sample; and T_r represents the transpose of a matrix.

The output training vector, Y, is expressed as follows.

$$Y = \begin{bmatrix} E_t^{*1} & E_t^{*2} & \cdots & E_t^{*n} \end{bmatrix}^{T_r}, \tag{20}$$

where E_t^{*n} is the energy level at current time step for the nth sample.

Both the input and output training matrices of (19) and (20) are calculated using (1)–(16). The energy level, charging power/discharging power, and SoC are varied randomly using uniform distribution functions to generate the training data set.

Since the ReLU activation function is represented as $f(.) = \max(0, .)$, the upper bound for the ReLU activation function is set as $E^{n,\max}$. Therefore, the mathematical model of the used NN is expressed as follows.

$$\hat{E}_t^n = x^n \cdot W + b, \tag{21}$$

$$E_t^n = \min(\max(0, \hat{E}_t^n), E^{n,\max}), \tag{22}$$

where W and b are the matrix and vector for weights and biases, respectively; and E_t^n is the predicted output by the NN. The initial weights and biases are randomly selected using Standard Gaussian distribution. The mean square error between actual and predicted outputs are minimized to train the NN using,

$$\min_{W,b} \frac{1}{n} \sum_{k=1}^{n} (E_t^n - E_t^{*n})^2. \tag{23}$$

2.2.2. Training algorithm for the NN with linear activation function to capture relationship between SoC and charging/discharging power limits

The input training vector to capture the relationship between SoC and charging/discharging limits using an NN with linear activation function is as follows.

$$A = \begin{bmatrix} SoC_t^1 & SoC_t^2 & \cdots & SoC_t^m \end{bmatrix}^{T_r}, \tag{24}$$

where A is the training input matrix and SoC_t^m is the SoC of the mth sample.

The labeled output training vector, B, is given in (25).

$$B = \begin{bmatrix} P_t^{*,\max,1} & P_t^{*,\max,2} & \cdots & P_t^{*,\max,m} \end{bmatrix}^{T_r}, \tag{25}$$

The symbol $*$ is replaced by charging or discharging based on the scope of implementation.

The expression to calculate charging/discharging power limits from SoC based on linear activation function is as follows.

$$P_m^{*,\max*} = SoC_t^m W^* + b^*, \tag{26}$$

where W^* and b^* are weights and biases, respectively and $P_m^{*,\max*}$ is the predicted charging/discharging power limits by the NN. To train the NN, the mean square error is minimized as follows.

$$\min_{W^*,b^*} \frac{1}{m} \sum_{l=1}^{m} (P_m^{*,\max*} - P_m^{*,\max})^2, \tag{27}$$

2.3. Mathematical model for the proposed battery model

After training the NNs, a mathematical representation using the weights and biases of the trained networks is developed to avoid the requirement of non-linear equations to capture battery characteristics. In this model, the expression to calculate the energy level at current time step is as follows.

$$E_t^n = \min(E_t^{n,temp}, E^{n,\max}) \tag{28}$$

$$E_t^{n,temp} = \max(\hat{E}_t^n, E^{n,\min}) \tag{29}$$

Subjected to the following constraints,

$$E^{n,\min} \le E_t^{n,temp} \le E^{n,\min} + (1 - Z_{1,t})M, \tag{30}$$

$$\hat{E}_t^n \le E_t^{n,temp} \le \hat{E}_t^n + Z_{1,t} M, \tag{31}$$

$$E^{n,\max} - (1 - Z_{2,t})M \le E_t^n \le E^{n,\max}, \tag{32}$$

$$E_t^{n,temp} - Z_{2,t} M \le E_t^n \le E_t^{n,temp}, \tag{33}$$

$$Z_{1,t} \in \{0, 1\}, \tag{34}$$

$$Z_{2,t} \in \{0, 1\}, \tag{35}$$

where $Z_{1,t}$ and $Z_{2,t}$, are introduced integer variables to represent decision of including an edge in a graph; $E_t^{n,temp}$ is the calculated energy level between maximum and minimum energy limits of the battery using (28)–(35) at time t for the n^th sample; and M is a sufficiently large number to ensure validity of the inequality constraints for all values of the integers variables.

The derived mathematical model explains the behavior of the battery model under charging and discharging conditions. If the value of $\hat{E}_t^n$ becomes less than $E^{n,\min}$ due to discharging, then (29) and (30) force $Z_{1,t}$ to be one. Consequently, (28) and (30) keep $E_t^n = E^{n,\min}$. On the other hand, if the value of $\hat{E}_t^n$ becomes more than $E^{n,\min}$ after charging/discharging, then (29) and (30) force $Z_{1,t}$ to be zero, and (28) and (31) keep $E_t^{n,temp} = \hat{E}_t^n$. Similarly, if $\hat{E}_t^n$ is more than $E^{n,\max}$ for charging then (29) and (32) force $Z_{2,t}$ to be one. Therefore, E_t^n becomes $E^{n,\max}$ by (28) and (33). If the $E_t^{n,temp}$ is less than $E^{n,\max}$ for charging/discharging then (28) and (32) force $Z_{2,t}$ to be zero, and E_t^n becomes $E_t^{n,temp}$ by (28) and (33).

3. Integrating the proposed battery model in power system reliability evaluation

This section explains the integration procedure of the developed battery model into power system reliability evaluation and enhancement. In the power system reliability studies, a power flow is solved to solve the optimization problem of minimizing load curtailments. In this paper, a linearized AC power flow formulation described in [29] and mixed integer linear programming are leveraged to formulate the objective function and network constraints with the proposed battery model.

3.1. Objective function

The objective function to minimize load curtailments is formulated as follows.

$$\mathcal{L}_d^{c,\min} = \min\left(\sum_{n^b \in N^b}^{Y} (L_{n^b,Y,d}^{c,a} + L_{n^b,Y,d}^{c,r})\right), \quad \forall d \tag{36}$$

where d is an indicator for a day in the year; Y is the total number of simulation years; N^b is the set for all buses; $L_{n^b,Y,d}^{c,a}$ and $L_{n^b,Y,d}^{c,r}$ are the active and reactive load curtailments of a power system on dth day of Yth year at bus n^b; and $\mathcal{L}_d^{c,\min}$ is the minimum amount of load curtailment of a power system on the dth day.

3.2. Network constraints

The network constraints to solve the optimization problem given in (36) are explained as follows.

3.2.1. Power balance equations

The power balance at time t on a day d can be expressed as follows.

$$\begin{aligned} B'_{t,d}\theta_{t,d} - G_{t,d}V_{t,d} + P_{t,d}^{g} + P_{t,d}^{dis} + L_{t,d}^{c,a} \\ = P_{t,d}^{l} + P_{t,d}^{ch}, \ \forall t, \forall d, \end{aligned} \tag{37}$$

$$G'_{t,d}\theta_{t,d} + B_{t,d}V_{t,d} + Q_{t,d}^{g} + L_{t,d}^{c,r} = Q_{t,d}^{l}, \quad \forall t, \forall d, \tag{38}$$

where t is the index for hours of a day, running from 1 to 24; $B'_{t,d}$ and $G'_{t,d}$ are the modified susceptance and conductance matrices [29], respectively; $B_{t,d}$ is the conventional susceptance matrix; $G_{t,d}$ is the conventional conductance matrix; $\theta_{t,d}$ is the vector of nodal voltage angles; $V_{t,d}$ is the vector of nodal voltage magnitudes; $P_{t,d}^{g}$ is the vector of real power generation; $Q_{t,d}^{g}$ is the vector of reactive power generation; $P_{t,d}^{dis}$ is the vector for discharging power of batteries; $P_{t,d}^{ch}$ is the vector for charging power of batteries; $P_{t,d}^{l}$ is the vector for real power demand; $Q_{t,d}^{l}$ is the vector for reactive power demand; $L_{t,d}^{a,r}$ is the vector of active load curtailment; and $L_{t,d}^{c,r}$ is the vector of reactive load curtailment.

3.2.2. Battery model equality constraints

The battery model, representing SoC and power values, at time t on day d is expressed as follows.

$$E_{t,d} = E_{t-1,d} - W(P_{t-1,d}^{dis} - P_{t,d}^{ch}) + b, \quad \forall t, \forall d, \tag{39}$$

$$P_{t,d}^{dis,\max} = W^{dm} SoC_{t,d} + b^{dm}, \quad \forall t, \forall d, \tag{40}$$

$$P_{t,d}^{ch,\max} = W^{cm} SoC_{t,d} + b^{cm}, \quad \forall t, \forall d, \tag{41}$$

where $E_{t-1,d}$ is the battery energy level before charging/discharging; $E_{t,d}$ is the battery energy level after charging/discharging; W and b are the weights and biases of the trained NN obtained using (19)–(23); $SoC_{t,d}$ is the battery SoC; $P_{t,d}^{dis,\max}$ is the maximum discharging power; $P_{t,d}^{ch,\max}$ is the maximum charging power; W^{dm} and b^{dm} are the weights and biases for discharging, respectively; and W^{cm} and b^{cm} are the weights and biases for charging which are obtained from the trained NN based on (24)–(27).

3.2.3. Battery model inequality constraints

The mathematical model introduced in Section 2.3 is used to derive the inequality constraints for battery model in reliability evaluation problems as follows.

$$E^{\min} \le E_{t,d}^{temp} \le E^{\min} + (1 - Z_{1,t,d})M, \quad \forall t, \forall d, \tag{42}$$

$$\hat{E}_{t,d} \le E_{t,d}^{temp} \le \hat{E}_{t,d} + Z_{1,t,d}M, \quad \forall t, \forall d, \tag{43}$$

$$E^{\max} - (1 - Z_{2,t,d}) \le E_{t,d} \le E^{\max}, \quad \forall t, \forall d, \tag{44}$$

$$E_{t,d}^{temp} - Z_{2,t,d}M \le E_{t,d} \le E_{t,d}^{temp}, \quad \forall t, \forall d, \tag{45}$$

$$Z_{1,t,d} \in \{0, 1\}, \quad \forall t, \forall d, \tag{46}$$

$$Z_{2,t,d} \in \{0, 1\}, \quad \forall t, \forall d. \tag{47}$$

3.2.4. Charging/discharging power limits

The battery charging and discharging power limits at time t on day d must be within the battery capacity, which are expressed as follows,

$$0 \le P_{t,d}^{ch} \le P_{t,d}^{ch,\max}, \quad \forall t, \forall d, \tag{48}$$

$$0 \le P_{t,d}^{dis} \le P_{t,d}^{dis,\max}, \quad \forall t, \forall d. \tag{49}$$

3.2.5. Generation power limits

The generated power of all generators at time t on day d is as follows.

$$P_g^{\min} \le P_{t,d}^{g} \le P_g^{\max}, \quad \forall t, \forall d, \tag{50}$$

$$Q_g^{\min} \le Q_{t,d}^{g} \le Q_g^{\max}, \quad \forall t, \forall d, \tag{51}$$

where $P_g^{\min}$ is the vector of minimum real power generation; $P_g^{\max}$ is the vector of maximum real power generation; $Q_g^{\min}$ is the vector of minimum reactive power generation; and $Q_g^{\max}$ is the vectors of maximum reactive power generation.

3.2.6. Load curtailment limits

The amount of load curtailment at each bus should be less than or equal to the total amount of load at the same bus for a specific time t on day d, which are expressed as follows.

$$0 \le L_{t,d}^{c,a} \le P_{t,d}^{l}, \quad \forall t, \forall d, \tag{52}$$

$$0 \le L_{t,d}^{c,r} \le Q_{t,d}^{l}, \quad \forall t, \forall d. \tag{53}$$

3.2.7. Feeder capacity constraints

The forward and reverse power flows through a specific line connected at any time t on day d must be within line capacities, which are expressed as follows.

$$S_{t,d}^{F} \le S_F^{\max}, \quad \forall t, \forall d, \tag{54}$$

$$-S_{t,d}^{R} \le S_R^{\max}, \quad \forall t, \forall d, \tag{55}$$

where $S_F^{\max}$ is the vector of maximum forward line flow capacities; $S_R^{\max}$ is the vector of maximum reverse line flow capacities; $S_{t,d}^{F}$ is the vector of forward line flows; and $S_{t,d}^{R}$ is the vector of reverse line flows.

3.2.8. Voltage limits

Voltage magnitudes for all buses at time t on day d can be expressed as follows.

$$V^{\min} \le V_{t,d} \le V^{\max}, \quad \forall t, \forall d, \tag{56}$$

where $V^{\min}$ is the vector of minimum bus voltage magnitudes; and $V^{\max}$ is the vector of maximum bus voltage magnitudes.

3.2.9. Angle limits

Voltage angles for all buses at time t on day d can be expressed as follows.

$$-\pi \leq \theta_{t,d}, \leq \pi \quad \forall t, \forall d. \tag{57}$$

3.3. Reliability evaluation index

In reliability evaluation studies of power systems, the energy indices have been observed as the slowest indices in terms of convergence using Monte Carlo Simulation [30]. Therefore, the expected demand not supplied (EDNS) index is calculated in this work. It is worth mentioning here that the operators will also have the flexibility to choose other reliability indices for evaluating reliability of power systems with the proposed battery model. The EDNS is expressed as follows.

$$EDNS = \left(\frac{1}{(8760 \times Y)} \sum_{y=1}^{Y} \mathcal{L}_{d,y}^{c,\min} \right), \tag{58}$$

where Y is the total number simulated years; and $L_{d,y}^{c,\min}$ is the amount of minimum load curtailments on day d of year y.

4. Optimal battery locations for reliability maximization

This section describes the criteria used to evaluate optimal locations for batteries to enhance reliability of power systems considering the proposed battery model.

4.1. Evaluation criteria

To achieve efficient utilization of batteries in power systems, an optimal battery siting strategy needs to be developed. In this work, we have focused on determining optimal battery locations to maximize power system reliability. The EDNS and Energy Index of Reliability (EIR) are used to determine optimal locations for batteries. The ability of both indices to capture the severity of expected power system outages makes them good candidates for reliability evaluation criteria. The EIR is calculated as follows.

$$EIR = 1 - \frac{EDNS \times 8760}{E_{Total}}, \tag{59}$$

where E_{Total} is the total amount of required energy in each year.

The value of EIR provides an indicator for the reliability level. For instance, a perfectly reliable system (EDNS = 0) has EIR value of one, whereas the EIR value reduces if EDNS is greater than zero. In other words, the value of EIR is inversely proportional of EDNS (reliability decreases as well). Therefore, we need to maximize the EIR via determining optimal locations for batteries to enhance the reliability of power systems. If the total number of possible deployment sites is m_{bt} for a specific number of batteries, N^{bt}, then the decision to locate the batteries can be represented using m_{bt} binary bits. Thus, a binary string, X, with m_{bt} bits can be used to encode the variables. The mathematical model to represent the optimization problem is expressed as follows.

$$\max f = \mathrm{EIR}(X), \tag{60}$$

$$\text{Subject to, } \sum_{i^{bt}=1}^{m_{bt}} X_{i^{bt}} \leq N^{bt}, \tag{61}$$

where X is the binary string.

4.2. The algorithm to determine optimal battery locations

As there could be several feasible sites, the optimal sites that maximize EIR are searched through GA. Determining optimal locations of battery energy storage systems requires repetitively running the simulations for a large number of scenarios. This exhaustive search could take a very long time (days to months depending on system sizes) to obtain the complete solution. In [31], GA has been used for optimal siting and sizing of distributed generators with storage systems using feeder reconfiguration. In [32], optimal sites and sizes for utility-scale shared energy storage systems with high solar penetration have been determined using GA. In [33], GA has been used to solve generation expansion planning problems. GA has been used to solve electric distribution service restoration through minimizing out-of service area, switching operation, and power loss [34]. Following the same convention of [31–34], GA is adopted to find the optimal or near optimal battery locations. In the GA, the variables are represented by chromosomes which are composed of genes. Several steps such as reproduction, crossover, and mutation are conducted iteratively among chromosomes to reach the best fitness. A solution is obtained by either converging to a best fitness value or reaching the maximum number of iterations [35].

The detailed procedure to determine the optimal battery locations for reliability maximization problem using GA algorithm is illustrated as follows.

1. **Develop Battery Model:** Construct an equivalent battery model using electrochemical properties based on Section 2.1.
2. **Capturing Non-linear Battery Characteristics:** Train an NN with ReLU activation function to capture the relationship between battery energy level and charging/discharging power based on the procedure described in Section 2.2.1. Also, train two NNs with a linear activation function separately to establish relationship between SoC, charging power limits, and discharging power limits based on Section 2.2.2.
3. **Battery Mathematical Model:** Extract all the weights and biases of the trained NNs. Then, formulate a mathematical model incorporating integer variables for the proposed NN-based battery model using the procedure described in 2.3.
4. **Reliability Evaluation Formulation:** Integrate the developed NN-based battery model into reliability evaluation problem based on Section 3.
5. **Optimal Battery Locations:** Determine the optimal sites for battery units to enhance the reliability of power systems using GA based on Section 4.1.

The architecture to both develop and integrate the proposed battery model in probabilistic analyses is shown in Fig. 2.

5. Implementation and results

To validate the proposed method, simulations are carried out on a modified version of the IEEE 33-bus distribution system. The IEEE 33-bus test system consists of 33 nodes, 32 branches, 5 tie-lines, 3 laterals, and the operating voltage is 12.66 kV [36]. In the modified IEEE 33-bus system, locations of the generating units and ratings of the photovoltaic (PV) units are selected based on the provided modification in [37]. The total peak demand of the modified 33-bus test system is 2972 kW [37]. The limits of hourly generation amount of PV units are calculated using PVWatts calculator developed by the US National Renewable Energy Laboratory [38]. The rating of each battery is taken from [6], which is 5.32 kWh and we assume that 10 batteries are aggregated to install at each selected location. Thus, the aggregated capacity of the batteries to be installed is 53.20 kWh. The locations of the DGs in the modified IEEE 33-bus distribution system are shown in Fig. 3. The ratings of all the DGs are given in Table 1.

Three different case studies are carried out to demonstrate the proposed method, which are as follows.

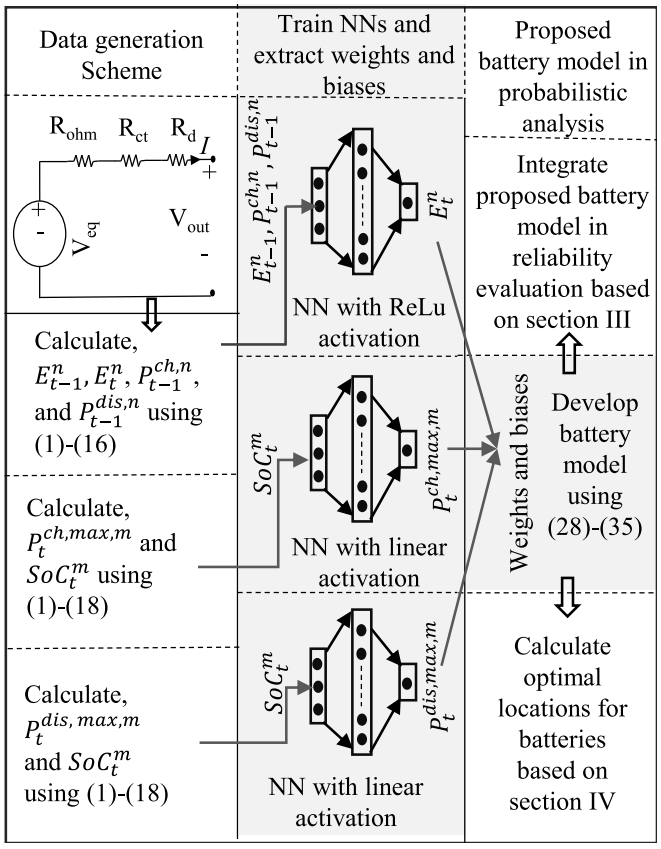

Fig. 2. Architecture to develop and integrate the proposed battery model in probabilistic analyses.

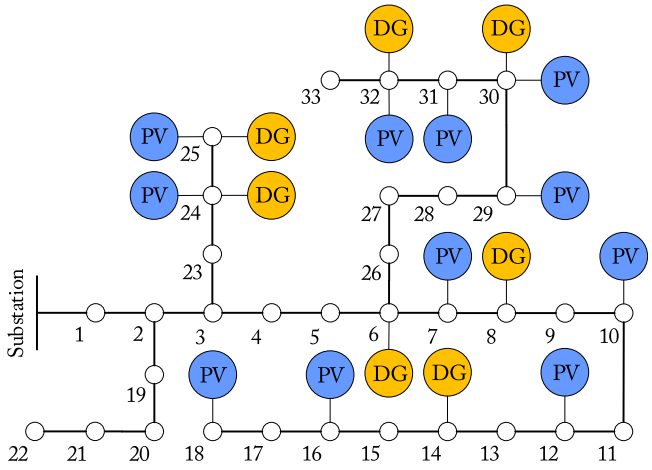

Fig. 3. Modified IEEE 33-bus distribution system.

- **Case I:** Comparative study between equivalent battery circuit model and machine learning-based battery model.
- **Case II:** Analyzing the impacts of the accurate battery model on reliability of power systems.
- **Case III:** Analyzing the impacts of accurate battery model in determining optimal battery sites.

The above mentioned case studies are described as follows.

Case I:. In this case, the accuracy of predicted next state energy level and charging/discharging power limits of the trained NNs are analyzed. From the experimental results provided in [6], it is observed that the discharging efficiency of Li-ion batteries is low at low SoC level, whereas the charging efficiency is low at high SoC level. Therefore, we assume that the permissible SoC levels of batteries for charging/discharging are 25–95%.

Table 1
Ratings of generators of the modified IEEE 33-bus.

Types of generators	Locations (Node No.)	Rating (kW)	Types of generators	Locations (nod No.)	Rating (kW)
DG	6	1200	PV	12	50
DG	8	400	PV	16	50
DG	14	400	PV	18	100
DG	24	800	PV	24	300
DG	25	800	PV	25	250
DG	30	400	PV	29	100
DG	32	400	PV	30	200
PV	7	100	PV	31	150
PV	10	100	PV	32	50

To predict next state energy level using current state energy level and charging/discharging power, a single layer NN with an ReLU activation function is trained based on the approach described in section 2.2.1. The input training data and labeled target data are randomly sampled for different SoC levels using (1)–(20). Total of 1000 samples are used to train the network. Among these samples, 70% are used for training and 30% are used for testing. To demonstrate the effectiveness of the trained network, a snapshot of the predicted results by the trained network for 50 randomly selected input samples (current state energy level and charging/discharging power) and the results of experimentally validated equivalent circuit model for the same inputs are shown in Fig. 4.

From Fig. 4, it can be seen that the difference between the results obtained using the trained network and experimentally validated circuit model is almost zero. Thus, it can be claimed that the proposed NN-based battery model can precisely emulate the results of experimentally validated circuit model.

To predict charging power limits from SoC levels, a single layer NN with linear activation function is trained based on Section 2.2.2. The training samples for different random SoC levels are generated using (17), (24), and (25). The total number of training samples for this scenario is also 1000. Similarly, 70% of these samples are used for training and remaining 30% are used for testing. To demonstrate effectiveness of the trained network, a snapshot of the predicted charging power limits by the trained NN and calculated charging power limits using equivalent battery circuit model for 25 different SoC levels is shown in Fig. 5.

Similar to charging power limits and SoC, a single layer NN with linear activation function is trained based on Section 2.2.2 to predict the discharging power limits from SoC levels. The training samples for different random SoC levels are generated using (18), (24), and (25). Also, the total number of training samples for this scenario is 1000, and 70% of these samples are used for training and remaining 30% are used for testing. Also, a snapshot for the predicted discharging power limits of the trained NN for 25 different SoC levels and calculated discharging power limits using (18) based on the equivalent circuit model for the same SoC levels are shown in Fig. 6.

From Figs. 5 and 6, we can see that the trained networks for both charging and discharging power limits are capable to mimic the results of experimentally validated circuit model.

Case II:. In this case, the reliability of the modified IEEE 33-bus distribution system is calculated using both the proposed accurate battery model and ideal battery model. Two aggregated batteries are installed at two randomly selected buses (i.e., bus no. 24 and 30). The algorithm described in Section 3 is used to evaluate the reliability with accurate battery models. The reliability with ideal battery model is calculated

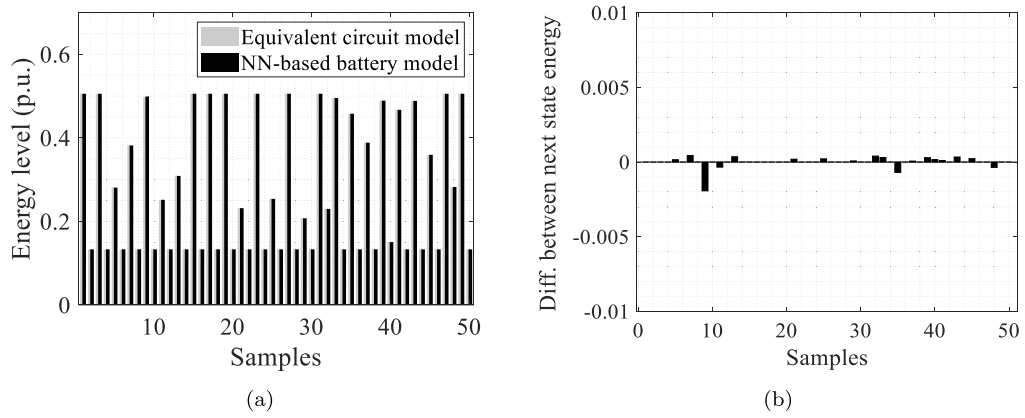

Fig. 4. Calculated (a) next state energy and (b) difference between next state energy using equivalent circuit model and neural network.

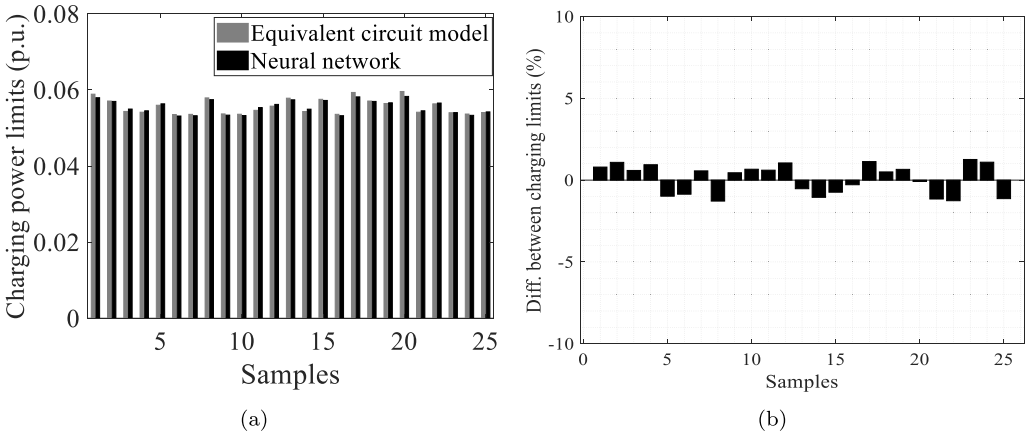

Fig. 5. (a) Charging power limits and (b) difference between charging power limits for equivalent circuit model and neural network.

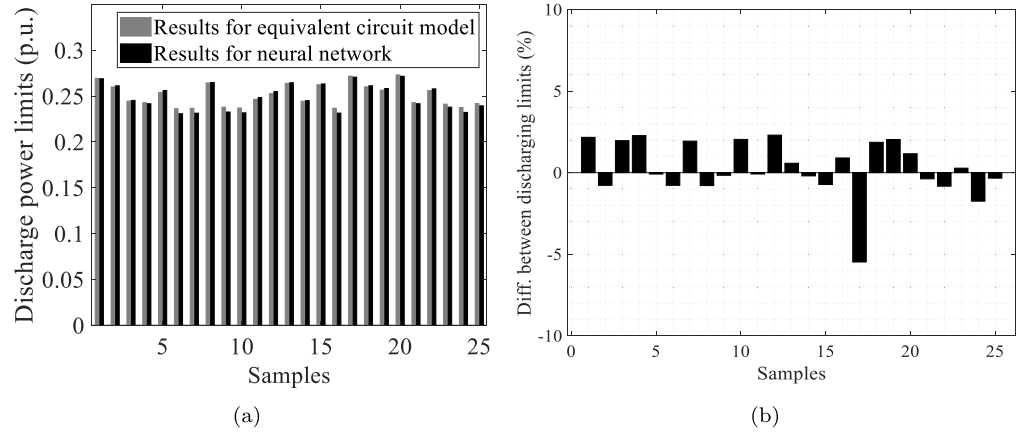

Fig. 6. Calculated (a) discharging power limits and (b) difference between discharging power limits using equivalent circuit model and neural network.

to analyze the impacts of the accurate battery model on power system reliability evaluation. In [39,40], the charging/discharging efficiencies for the ideal battery model have been varied from 85%–95%. Following the same convention, both charging and discharging efficiencies are considered constant (95%) for the ideal battery model. The results for the accurate and ideal battery models are shown in Table 2.

From Table 2, it can be seen that the EDNS with accurate model is approximately 17.41% larger than that of ideal battery model. Therefore, inclusion of the accurate battery model in the reliability evaluation methods is important to achieve accurate results.

Table 2
Reliability index of the modified IEEE 33-bus.

Scenarios	EDNS (kW/year)
With NN-based battery model	5.41196
With ideal battery model	4.61579

Case III:. In this case, the optimal locations to install batteries to enhance the reliability are determined based on the procedure described in Section 4 using both the accurate and ideal battery models. Similar

Table 3
Optimal locations for batteries to maximize reliability of the modified IEEE 33-bus.

Scenarios	Battery locations (Bus No.)	EDNS (kW/year)
With ideal battery model	7, 24	3.70451
With NN-based battery model	8, 7	3.29342

to [36], we assume that two optimal locations from six candidate buses will be determined to install two aggregated batteries to enhance reliability of the modified IEEE 33-bus distribution system. The candidate buses are 7, 8, 24, 25, 30, and 32 [36]. The decision of installing the batteries in the selected buses are represented using binary strings. The determined optimal locations for the accurate and ideal battery models with respective EDNS values are shown in Table 3. In the above case studies, we have presented results for maximizing the expected index of reliability. In other words, we investigated the impacts of the actual battery model on determining optimal battery locations to minimize expected load curtailment. From the results of Tables 2 and 3, we can see that optimal battery locations for ideal battery models are different from the proposed actual battery model. This indicates that using ideal battery models the results will be conservative (as shown in Table 3). In addition to being computationally attractive, the proposed model provides more accurate results. Therefore, it can be concluded that the proposed battery model can play a vital role in determining accurate optimal battery locations to maximize reliability of power systems.

It is worth mentioning here that the proposed battery model can be realized into practical power systems with the knowledge of system characteristics such as number of nodes and branches, number of tie lines, operating voltages, generation capacity, load profile, availability of system equipment, candidate locations etc., which can be a great future research scope. To incorporate the proposed data-driven battery model into probabilistic analysis of practical power systems, first, NNs need to be trained to establish actual relationships between charging/discharging power and energy and charging/discharging power limits and SoC of batteries based on the proposed approach in Sections 2.1 and 2.2. Then, weights and biases of the trained networks and MILP need to be used to formulate a mathematical model for the proposed battery model based on Section 2.3.

Also, in this work, *Case I* validates the effectiveness of the proposed battery model in emulating the characteristics of analytical/accurate battery models. Comparative results between ideal battery models and proposed battery models are provided in *Case II* and *Case III* to demonstrate the impacts of actual battery models on the obtained results compared to the ideal battery models. The comparative study between the proposed battery model and analytical battery models for computational speed can be a future scope of research.

6. Conclusion

This paper has proposed a machine learning-based battery model to capture actual battery characteristics without solving a set of non-linear equations. The non-linear relationship between battery energy level and charging/discharging power has been captured using an NN with ReLU activation function whereas an NN with linear activation function has been used to capture the relationship between SoC and charging/discharging power limits. Also, a mathematical model has been developed using mixed integer linear programming, weights and biases of the trained NNs, and a linearized AC power flow model to capture the time-synchronized relationship between charging/discharging power and energy level of batteries in the reliability evaluation problem of power systems. Moreover, a GA-based approach is used to determine optimal locations for batteries to enhance reliability of power systems considering the proposed battery model. The proposed approach was demonstrated on a modified version of the IEEE 33-bus distribution system through several case studies. The results of these case studies showed that the developed machine learning-based battery model can mimic the characteristics of experimentally validated equivalent battery model. Also, the results showed that the accurate battery model has significant impacts on both reliability evaluation efforts and results of optimal battery siting.

CRediT authorship contribution statement

Md. Kamruzzaman: Methodology, Software, Writing – original draft. **Xiaohu Zhang:** Conceptualization, Methodology, Supervision. **Michael Abdelmalak:** Methodology. **Di Shi:** Writing – reviewing. **Mohammed Benidris:** Writing – review & editing.

Declaration of competing interest

The authors declare that they have no known competing financial interests or personal relationships that could have appeared to influence the work reported in this paper.

Acknowledgment

This work was supported by the U.S. National Science Foundation (NSF) under Grant NSF 1847578.

References

[1] D.M. Rosewater, D.A. Copp, T.A. Nguyen, R.H. Byrne, S. Santoso, Battery energy storage models for optimal control, IEEE Access 7 (2019) 178357–178391.
[2] M. Sitterly, L.Y. Wang, G.G. Yin, C. Wang, Enhanced identification of battery models for real-time battery management, IEEE Trans. Sustain. Energy 2 (3) (2011) 300–308.
[3] R. Ahmed, M.E. Sayed, I. Arasaratnam, J. Tjong, S. Habibi, Reduced-order electrochemical model parameters identification and state of charge estimation for healthy and aged Li-ion batteries—Part II: Aged battery model and state of charge estimation, IEEE J. Emerg. Sel. Top. Power Electron. 2 (3) (2014) 678–690.
[4] Y. Cao, R.C. Kroeze, P.T. Krein, Multi-timescale parametric electrical battery model for use in dynamic electric vehicle simulations, IEEE Trans. Transp. Electr. 2 (4) (2016) 432–442.
[5] M. Kwak, B. Lkhagvasuren, J. Park, J. You, Parameter identification and SoC estimation of a battery under the hysteresis effect, IEEE Trans. Ind. Electron. (2019) 1, http://dx.doi.org/10.1109/TIE.2019.2956394.
[6] Alberto Berrueta, Andoni Urtasun, Alfredo Ursúa, Pablo Sanchis, A comprehensive model for Lithium-ion batteries: From the physical principles to an electrical model, Energy 144 (2018) 286–300.
[7] A. Fotouhi, D.J. Auger, K. Propp, S. Longo, Accuracy versus simplicity in online battery model identification, IEEE Trans. Syst. Man Cybern. Syst. 48 (2) (2018) 195–206.
[8] H. Pandžić, V. Bobanac, An accurate charging model of battery energy storage, IEEE Trans. Power Syst. 34 (2) (2019) 1416–1426.
[9] Dickshon N.T. How, Mahammad A. Hannan, Molla S. Hossain Lipu, Khairul S.M. Sahari, Pin Jern Ker, Kashem M. Muttaqi, State-of-charge estimation of Li-ion battery in electric vehicles: A deep neural network approach, IEEE Trans. Ind. Appl. 56 (5) (2020) 5565–5574.
[10] Lei Ren, Jiabao Dong, Xiaokang Wang, Zihao Meng, Li Zhao, M. Jamal Deen, A data-driven auto-CNN-LSTM prediction model for Lithium-ion battery remaining useful life, IEEE Trans. Ind. Inf. 17 (5) (2021) 3478–3487.
[11] Wenwu Zhong, Zongpeng Wang, Nan Gao, Liangai Huang, Zhiping Lin, Yanping Liu, Fanqi Meng, Jun Deng, Shifeng Jin, Qinghua Zhang, et al., Coupled vacancy pairs in Ni-doped cose for improved electrocatalytic hydrogen production through topochemical deintercalation, Angewandte Chemie Int. Ed. 59 (50) (2020) 22743–22748.
[12] Zongpeng Wang, Zhiping Lin, Jun Deng, Shijie Shen, Fanqi Meng, Jitang Zhang, Qinghua Zhang, Wenwu Zhong, Lin Gu, Oxygen evolution reaction: Elevating the d-band center of six-coordinated octahedrons in Co9S8 through Fe-incorporated topochemical deintercalation (Adv. Energy Mater. 5/2021), Adv. Energy Mater. 11 (5) (2021) 1–7.
[13] Wenwu Zhong, Beibei Xiao, Zhiping Lin, Zongpeng Wang, Liangai Huang, Shijie Shen, Qinghua Zhang, Lin Gu, RhSe2: a superior 3D electrocatalyst with multiple active facets for hydrogen evolution reaction in both Acid and Alkaline solutions, Adv. Mater. 33 (9) (2021) 2007894.
[14] Shijie Shen, Zhiping Lin, Kai Song, Zongpeng Wang, Liangai Huang, Linghui Yan, Fanqi Meng, Qinghua Zhang, Lin Gu, Wenwu Zhong, Reversed active sites boost the intrinsic activity of graphene-like cobalt selenide for hydrogen evolution, Angewandte Chemie Int. Ed. 60 (22) (2021) 12360–12365.

[15] Zhiping Lin, Shijie Shen, Zongpeng Wang, Wenwu Zhong, Laser ablation in air and its application in catalytic water splitting and Li-ion battery, Iscience (2021) 102469.
[16] Z. Xi, M. Dahmardeh, B. Xia, Y. Fu, C. Mi, Learning of battery model bias for effective state of charge estimation of Lithium-ion batteries, IEEE Trans. Veh. Technol. 68 (9) (2019) 8613–8628.
[17] A.J. Gonzalez-Castellanos, D. Pozo, A. Bischi, Non-ideal linear operation model for Li-ion batteries, IEEE Trans. Power Syst. 35 (1) (2020) 672–682.
[18] Jiashen Teh, Ching-Ming Lai, Reliability impacts of the dynamic thermal rating and battery energy storage systems on wind-integrated power networks, Sustain. Energy Grids Netw. 20 (2019) 100268.
[19] Mohamed K. Metwaly, Jiashen Teh, Optimum network ageing and battery sizing for improved wind penetration and reliability, IEEE Access 8 (2020) 118603–118611, http://dx.doi.org/10.1109/ACCESS.2020.3005676.
[20] Mohamed Kamel Metwaly, Jiashen Teh, Probabilistic peak demand matching by battery energy storage alongside dynamic thermal ratings and demand response for enhanced network reliability, IEEE Access 8 (2020) 181547–181559, http://dx.doi.org/10.1109/ACCESS.2020.3024846.
[21] Kyung-Hee Jung, Hoyong Kim, Daeseok Rho, Determination of the installation site and optimal capacity of the battery energy storage system for load leveling, IEEE Trans. Energy Convers. 11 (1) (1996) 162–167.
[22] H. Mohsenian-Rad, Optimal bidding, scheduling, and deployment of battery systems in California day-ahead energy market, IEEE Trans. Power Syst. 31 (1) (2016) 442–453.
[23] Wong Ling Ai, Hussain Shareef, Ahmad Asrul Ibrahim, Azah Mohamed, Optimal battery placement in photovoltaic based distributed generation using binary firefly algorithm for voltage rise mitigation, in: IEEE International Conference on Power and Energy (PECon), Kuching, Malaysia, 2014, pp. 155–158.
[24] K. Khalid Mehmood, S.U. Khan, S. Lee, Z.M. Haider, M.K. Rafique, C. Kim, Optimal sizing and allocation of battery energy storage systems with wind and solar power DGs in a distribution network for voltage regulation considering the lifespan of batteries, IET Renew. Power Gener. 11 (10) (2017) 1305–1315.
[25] S. Shafiq, B. Khan, A.T. Al-Awami, Optimal battery placement in distribution network using voltage sensitivity approach, in: IEEE Power and Energy Conference At Illinois (PECI), Champaign, IL, USA, USA, 2019, pp. 1–4.
[26] A.A. Seijas, P.C. del Granado, H. Farahmand, J. Rueda, Optimal battery systems designs for Distribution Grids: What size and location to invest in? in: International Conference on Smart Energy Systems and Technologies (SEST), Sep., 2019, pp. 1–6.
[27] Farihan Mohamad, Jiashen Teh, Ching-Ming Lai, Optimum allocation of battery energy storage systems for power grid enhanced with solar energy, Energy 223 (2021) 120105.
[28] Samer Sulaeman, Yuting Tian, Mohammed Benidris, Joydeep Mitra, Quantification of storage necessary to firm up wind generation, IEEE Trans. Ind. Appl. 53 (4) (2017) 3228–3236.
[29] S. Elsaiah, M. Benidris, J. Mitra, Analytical approach for placement and sizing of distributed generation on distribution systems, IET Gen., Trans. & Dist. 8 (6) (2014) 1039–1049.
[30] R. Billinton, W. Li, Reliability Assessment of Electric Power Systems using Monte Carlo Methods, Plenum Press, Ney York, USA, 1994.
[31] Fazel Abbasi, Seyed Mehdi Hosseini, Optimal DG allocation and sizing in presence of storage systems considering network configuration effects in distribution systems, IET Generation Trans. Distribut. 10 (3) (2016) 617–624.
[32] Narayan Bhusal, Mukesh Gautam, Mohammed Benidris, Sushil J. Louis, Optimal sizing and siting of multi-purpose utility-scale shared energy storage systems, in: 52nd North American Power Symposium (NAPS), Tempe, AZ, USA, 2021, pp. 1–6.
[33] P. Murugan, S. Kannan, S. Baskar, Application of NSGA-II algorithm to single-objective transmission constrained generation expansion planning, IEEE Trans. Power Syst. 24 (4) (2009) 1790–1797.
[34] Yogendra Kumar, Biswarup Das, Jaydev Sharma, Multiobjective, multiconstraint service restoration of electric power distribution system with priority customers, IEEE Trans. Power Deliv. 23 (1) (2008) 261–270.
[35] J.H. Holland, Adaptation in Natural and Artificial Systems: An Introductory Analysis with Applications To Biology, Control, and Artificial Intelligence., MIT Press, 1992.
[36] S. Elsaiah, M. Benidris, J. Mitra, Reliability improvement of power distribution system through feeder reconfiguration, in: International Conference on Probabilistic Methods Applied To Power Systems, Durham, UK, 2014, pp. 1–6.
[37] C. Zhang, Y. Xu, Z.Y. Dong, Robustly coordinated operation of a multi-energy micro-grid in grid-connected and islanded modes under uncertainties, IEEE Trans. Sustain. Energy (2019) http://dx.doi.org/10.1109/TSTE.2019.2900082.
[38] National Renewable Energy Laboratory (NREL), NREL's PVWatts® calculator, 2018, URL https://pvwatts.nrel.gov/.
[39] Mohamed Alamgir, Ann Marie Sastry, Efficient batteries for transportation applications, in: Proceedings SAE Converge, 2008.
[40] X. Wang, Y. Hou, Y. Zhu, Y. Wu, R. Holze, An aqueous rechargeable lithium battery using coated li metal as anode, Sci. Rep. 3 (1401) (2013).